European Polymer Journal 46 (2010) 456–464

Contents lists available at ScienceDirect

European Polymer Journal

journal homepage: www.elsevier.com/locate/europolj

Polymorphism of the co-crystalline forms of syndiotactic polystyrene with chloroform: Crystal structure of the δ clathrate

Oreste Tarallo *, Maria Maddalena Schiavone, Vittorio Petraccone

Dipartimento di Chimica "Paolo Corradini", Università degli Studi di Napoli Federico II, Complesso di Monte S. Angelo, via Cintia, 80126 Napoli, Italy

ARTICLE INFO

Article history:
Received 27 October 2009
Received in revised form 10 December 2009
Accepted 13 December 2009
Available online 21 December 2009

Keywords:
Syndiotactic polystyrene
Clathrate
Chloroform
Crystal structure
X-ray diffraction

ABSTRACT

The crystal structure of the δ clathrate form of syndiotactic polystyrene (s-PS) containing $CHCl_3$, a molecule having a pivotal role in respect to the co-crystalline phases formation of this polymer, has been determined through X-ray diffraction data and molecular mechanics calculations. Analogously to all the other δ clathrate forms of s-PS, this structure presents a monoclinic unit cell (cell constants $a = 1.77$ nm, $b = 1.32$ nm, $c = 0.78$ nm and $\gamma = 121.5°$) in which the s(2/1)2 polymer helices and guest molecules are packed according the space group $P2_1/a$. At variance with all the other δ clathrate forms of s-PS whose crystal structure has been reported in the literature, probably due to the not planar shape of the chloroform guest molecule, in this structure guest molecules occupy each centrosymmetric cavity in a very low efficient way, giving rise to a disorder in the positioning of the guest molecules along the $b + a/2$ direction of the unit cell. A comparison with the ε type clathrate with the same guest, for which some preliminary results have been reported too, is also presented.

1. Introduction

Syndiotactic polystyrene (s-PS) is able to form different kinds of co-crystalline phases with a large number of guest molecules [1–13]. All of these exhibit an s(2/1)2 helical polymer conformation, with a repetition period of nearly 0.78 nm. These co-crystals can be obtained by guest sorption in the nanoporous δ [14] or ε [15,16] phase (see Fig. 1).

Semicrystalline s-PS samples exhibiting the nanoporous δ- and ε-crystalline phases can in fact rapidly and selectively absorb low molecular weight compounds both from gas phase and solutions even when present at very low concentrations. As a consequence, a number of applications in the field of chemical separations and of molecular sensorics has been proposed [17,18]. Moreover, the sorption of suitable guest molecules into these nanoporous phases leads to the formation of clathrate phases, which may display interesting properties depending on the guest molecule: for example, films presenting s-PS/active-guest co-crystals have been proposed as advanced chromophore [19], fluorescent [20], nonlinear optical [21], photoreactive [22], and magnetic materials [23].

s-PS co-crystalline phases can be divided in δ type co-crystals and ε type co-crystals, depending on their structure and on the starting nanoporous from which are obtained.

δ type co-crystals, in turn, can be divided in two classes. In the first one, defined as δ clathrates, guest molecules are imprisoned into isolated cavities cooperatively generated by two enantiomorphous helices of two adjacent *ac* layers of close packed polymer chains typical of the nanoporous δ form, as shown in Fig. 1 [14]. These clathrates are generally characterized by a maximum guest/monomer-unit molar ratio 1/4 [2–7,11]. Here guest molecules are accommodated in the δ form by increasing the distance between the *ac* layers and/or shifting them along the *a* axis direction [7]. In these clathrates guests are arranged with their molecular planes nearly perpendicular to the helical axes. The second class of s-PS δ co-crystals, defined as interca-

* Corresponding author. Tel.: +39 081 674443; fax: +39 081 674090.
E-mail address: oreste.tarallo@unina.it (O. Tarallo).

0014-3057/$ - see front matter © 2009 Elsevier Ltd. All rights reserved.
doi:10.1016/j.eurpolymj.2009.12.011

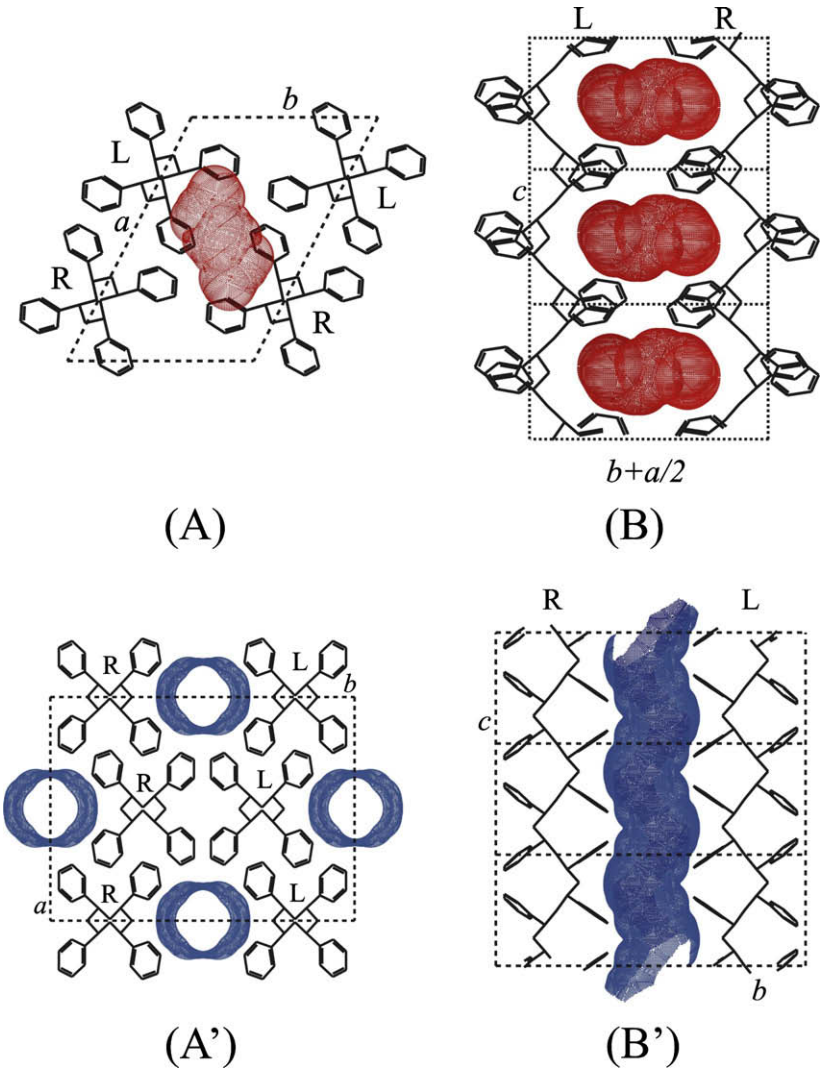

Fig. 1. Schematic representation of the nanoporous δ (A and B) and ε (A′ and B′) crystalline phases of s-PS: (A and A′) projections along the *c* axis; (B, B′) projections perpendicular to the *c* axis. The shapes of the cavities and of the channels (determined by the Connolly methods with a probe radius of 0.17 nm) are reported in red and blue, respectively. In (B) and (B′) only one couple of polymer chains delimiting the cavities are reported. R = right-handed, L = left-handed helical chains. (For interpretation of color mentioned in this figure the reader is referred to the web version of the article.)

lates, is characterized by the same *ac* layers of helices alternated to layers of guest molecules in which molecules are not isolated but contiguous. These structures generally present a maximum guest/monomer-unit molar ratio of 1/2 [8–10].

As far as ε type co-crystals, guest molecules are imprisoned into channels passing the unit cells of the ε form from side to side along the *c* direction (see Fig. 1) [15,16]. These co-crystals have been defined as ε clathrates. They are able to host different types of molecules, also with a molecular volume higher than those that can be hosted in the δ clathrates and also longer than the repetition period of the helices [15].

As far as the obtainment of the nanoporous δ and ε form, these can be only prepared by removing the guest from co-crystalline phases obtained in turn by treating with suitable solvents s-PS in amorphous samples or in *trans*-planar mesomorphous phase or in α and γ crystalline forms [12].

With regard to this fact it is worth pointing out the pivotal role of the chloroform molecule since, up to now, it is the only guest able to give rise to an ε co-crystal by exposure of samples in the γ form to liquid/vapor $CHCl_3$ [15,16]. The nanoporous ε form, essential for the obtainment of all the other ε co-crystals containing guest different from $CHCl_3$, can be obtained only by removing the guests from this co-crystal.

As far as the δ type co-crystalline phase with chloroform, it can be unfailingly obtained by exposure to $CHCl_3$ of amorphous or of oriented and unoriented α form samples.

$CHCl_3$ treatment of oriented or unoriented *trans*-planar mesomorphic specimens, instead, gives rise to samples containing a variable amount of both δ and ε clathrate

forms, generating in the literature some questions on the crystal structure of this co-crystalline form [2,13].

At the moment, the experimental conditions to obtain a pure ε or δ form starting from mesomorphic samples are still not well defined.

In order to understand the distinguishing behavior of this guest molecule in respect to the co-crystalline phases formation, it seemed interesting to us the investigation of the crystal structures of the s-PS δ and ε co-crystalline forms containing chloroform.

This contribution presents the detailed description of the crystalline structure of the s-PS δ clathrate form containing chloroform and some preliminary results on the ε co-crystalline form with the same guest.

2. Experimental part

The s-PS used in this study was manufactured (as pellets) by Dow Chemical Company under the trademark Questra 101. The ^{13}C nuclear magnetic resonance characterization showed that the content of syndiotactic triads was over 98%. The weight-average molar mass obtained by gel permeation chromatography (GPC) in trichlorobenzene at 135 °C was found to be $M_w = 3.2 \times 10^5$ with the dispersity index, $M_w/M_n = 3.9$.

Chloroform and CCl_4 were purchased from Aldrich and used without any further purification.

Oriented s-PS/$CHCl_3$ δ clathrate samples were obtained by exposure of oriented samples in the α form to liquid $CHCl_3$ at room temperature, keeping fixed the ends of the specimen. Fibers of the α form were obtained by drawing unoriented α form samples with a miniature mechanical tester apparatus (Reometric Scientific Minimat) at a drawing rate of 10 mm/min at a temperature in the range 105–110 °C. Unoriented α form specimens were prepared in a hot press by melting as supplied samples at 270° and successive rapid cooling.

Unoriented s-PS/$CHCl_3$ δ clathrate form samples were obtained by immersion in chloroform of powders in the crystalline δ form for 24–36 h at room temperature. Unoriented s-PS δ form samples were in turn obtained by removing (by acetone treatment) the guest from s-PS/toluene δ clathrate samples prepared by the dissolution in toluene of the as prepared pellets for 4 h.

The X-ray fiber diffraction patterns of oriented samples were obtained on a BAS-MS imaging plate (FUJIFILM) with a cylindrical camera (radius 57.3 mm, Ni-filtered Cu Kα radiation monochromatized with a graphite crystal) and processed with a digital scanner (FUJI-BAS 1800). Calculated intensities were obtained as $I_c = F_c^2 \cdot M_i \cdot B \cdot L_p$ were F_c is the calculated structure factor, M_i is the multiplicity, B is a thermal factor ($B = 12$ Å^2) and L_p is the Lorentz-polarization factor for X-ray fiber diffraction:

$$L_p = \frac{\left(\frac{0.5(\cos^2 2\theta + \cos^2 2\theta_M)}{1+\cos^2 2\theta_M} + \frac{0.5(1+\cos 2\theta_M \cos^2 2\theta)}{1+\cos 2\theta_M}\right)}{(\sin^2 2\theta - \varsigma^2)^{1/2}}$$

with $2\theta_M = 26.6°$ the inclination angle of the monochromator and $\zeta = \lambda(l/c)$, l and c being the order of the layer line and the chain axis periodicity, respectively, and λ the wavelength of the used radiation (1.5418 Å). Calculated structure factors were obtained as $F_c = (\sum |F_i|^2 M_i)^{1/2}$, where the summation is taken over all reflections included in the 2θ range of the corresponding spot observed in the X-ray fiber diffraction pattern. Atomic scattering factors from Ref. [24] were used. The observed intensities I_{obsd} were evaluated integrating the crystalline peaks observed in the X-ray diffraction profiles, read along different layer lines, after the subtraction of the background and amorphous contributions. Owing to the different shapes of the reflections on the equator and on the first and second layer lines, due to the different dimensions of the lamellar crystals in the direction perpendicular and parallel to the chain axis, different factors were used to scale the observed and calculated structure factors on the diverse layer lines. The discrepancy factor R has been evaluated as $R = \sum |F_{obsd} - F_{calcd}| / \sum F_{obsd}$ taking into account only the observed reflections.

Wide-angle X-ray diffraction patterns of unoriented samples were obtained with nickel-filtered Cu Kα radiation with an automatic Philips powder diffractometer operating in the $\theta/2\theta$ Bragg–Brentano geometry using 2 mm thick specimen holders.

Calculated X-ray powder diffraction pattern were obtained with the *Diffraction-Crystal* module of the software package *Cerius*^{2} (version 4.2 by *Accelrys Inc.*) using an isotropic thermal factor ($B = 12$ Å^2). A Gaussian profile function having a half-height width regulated by the average crystallite size along *a*, *b*, and *c* axes (L_a, L_b and L_c, respectively) was used. A good agreement with the half-height width of the peaks in the experimental profile has been obtained for $L_a = L_b = 10$ nm and $L_c = 8$ nm.

Energy calculations were carried out by using the Compass [25] force field within the *Open Force Field* module of *Cerius*^{2} by the smart minimizer method with standard convergence. The starting conformation of the s-PS polymer chains was that found by molecular mechanics calculations reported in the literature [26].

The shape and volume of the cavities, the volume of the polymer chains and the volume of the guest molecules have been determined with the *Connolly Surface* module of *Cerius*^{2} using a probe radius of 0.11 nm and a density dot of 0.1 nm^{-2} unless otherwise indicated.

3. Results and discussion

3.1. Crystal structure of the s-PS/$CHCl_3$ δ clathrate form

The X-ray fiber diffraction pattern of a uniaxially oriented sample of s-PS/$CHCl_3$ δ clathrate form is reported in Fig. 2A while Fig. 2B reports the X-ray diffraction pattern of an unoriented sample. All the reflections observed in the fiber diffraction patterns of Fig. 2A are listed in Table 1.

The experimental data reported in Table 1 can be well interpreted by a monoclinic unit cell with axes $a = 1.77$ nm, $b = 1.32$ nm, $c = 0.78$ nm and $\gamma = 121.5°$. The proposed space group is $P2_1/a$ in agreement with the systematic absence of *hk0* reflections with $h = 2n + 1$ and *00l* reflections with $l = 2n + 1$. The proposed unit cell is almost identical to that reported in the literature for the s-PS/toluene (and xylene) δ clathrate ($a = 1.76$ nm, $b = 1.33$ nm,

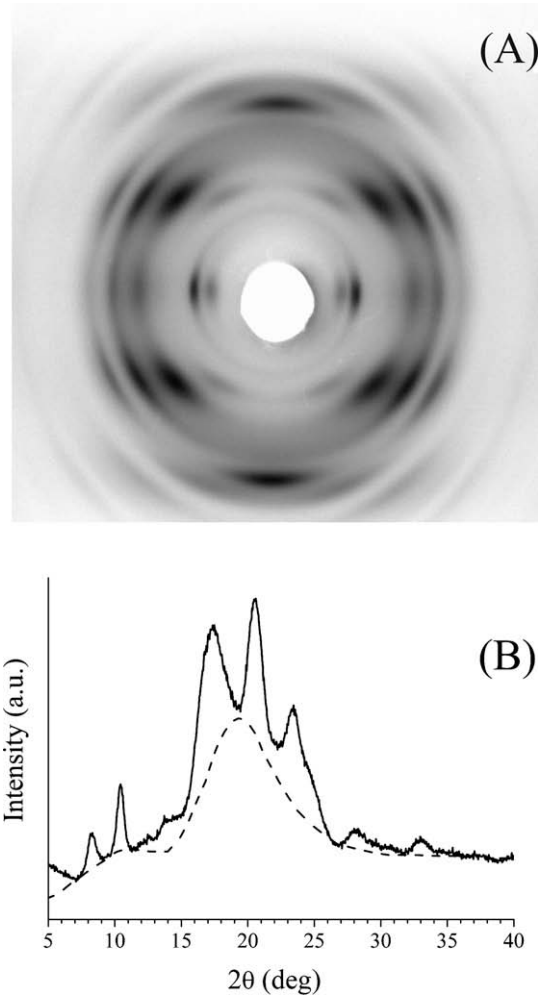

Fig. 2. X-ray diffraction pattern of an oriented (A) and unoriented (B) sample of the s-PS/$CHCl_3$ δ clathrate form. In (A) fiber axis is vertical. In (B) the amorphous and background contribution is indicated with a dashed line.

c = 0.77 nm and γ = 121.2°) [2] suggesting a structure isomorphous to those already found for other δ clathrates of s-PS.[1] We have then performed packing energy calculations assuming a $P2_1/a$ symmetry for the arrangement of the chains, keeping constant the unit cell parameters and optimizing the position of the guest molecule in the cavities. This arrangement of the chains creates centrosymmetric cavities where guest molecules, in principle, can be hosted according to two centrosymmetric orientations. Since the volume of the cavity generated by the polymer helices arranged as described before is ≈185 Å^3 while the $CHCl_3$ volume is ≈75 Å^3, in order to select promising structural models, we have performed minimizations examining either the possibility of arranging one or two guest molecules into each cavity. In the hypothesis of two guest molecules in each cavity, the minimum energy model obtained by maintaining the $P2_1/a$ symmetry for the whole crystal, is characterized by several distances between guests and polymer helices too short (0.33 nm). Consequently we abandoned this hypothesis, following also some literature data on chloroform equilibrium sorption [28]. In the hypothesis of one chloroform guest in each cavity, packing energy calculations were first performed for the arrangement of the only helices, assuming a $P2_1/a$ symmetry. Then, keeping fixed the helices in the situation of minimum energy found, we proceeded to the optimization of the position of the guest molecules inside the centrosymmetric cavities in the space group $P1$. Two nearly isoenergetic minimum energy arrangements of the guest were found (see Fig. 3) for which we performed structure factors calculations either as separated models or for their statistical combination (by introducing suitable occupancy factors for the $CHCl_3$ molecules).

Table 1
Diffraction angles ($2\theta_{obsd}$), Bragg distances (d_{obsd}) and intensities (I_{obsd}) in arbitrary units of the reflections observed on the layer lines (ℓ) in the X-ray fiber diffraction pattern of the s-PS/$CHCl_3$ δ clathrate form of Fig. 2A after the subtraction of the contribution of amorphous and background.

ℓ	$2\theta_{obsd}$ (°)	d_{obsd} (nm)	I_{obsd} (a.u.)
0	8.25	1.07	3300
0	10.2	0.87	8568
0	15.5	0.57	1222
0	17.4	0.51	5389
0	20.35	0.44	3058
0	23.2	0.38	1845
0	33.3	0.27	1393
1	13.7	0.65	5423
1	17.0	0.52	27808
1	20.2	0.44	14209
1	23.2	0.38	7336
1	32.4	0.28	1292
2	24.9	0.36	11504
2	27.9	0.32	4190
2	30.45	0.29	1399
2	32.9	0.27	1501

The best agreement between observed and calculated structure factors was obtained for a model in which there is only one guest molecule per each cavity statistically arranged according the four equivalent minimum energy positions indicated in Fig. 3. This could explain some IR data present in the literature indicating the existence of two distinct populations of guest molecules in the crystalline phase [29]. The discrepancy factor R between observed and calculated structure factor for the proposed model is 0.14. The fractional coordinates of its asymmetric unit are reported in Table 2. Table 3 reports the comparison between calculated and observed structure factors.

A further confirmation of the correctness of the proposed model is given in Fig. 4 where the X-ray powder diffraction profile calculated according to it is compared to the experimental X-ray powder diffraction pattern, after the subtraction of the amorphous and background contributions. A fairly good agreement is apparent.

Fig. 5 reports the detailed representation of the arrangement of the $CHCl_3$ molecules in the cavities of the s-PS/chloroform δ co-crystal structure found by molecular

[1] The similarity of the crystal lattice of s-PS/$CHCl_3$ clathrate with that proposed by Chatani et al. for the s-PS/toluene clathrate has been already suggested, on the basis of neutron diffraction patterns, by Daniel et al. in a paper on thermoreversible gelation of s-PS in toluene and chloroform [27].

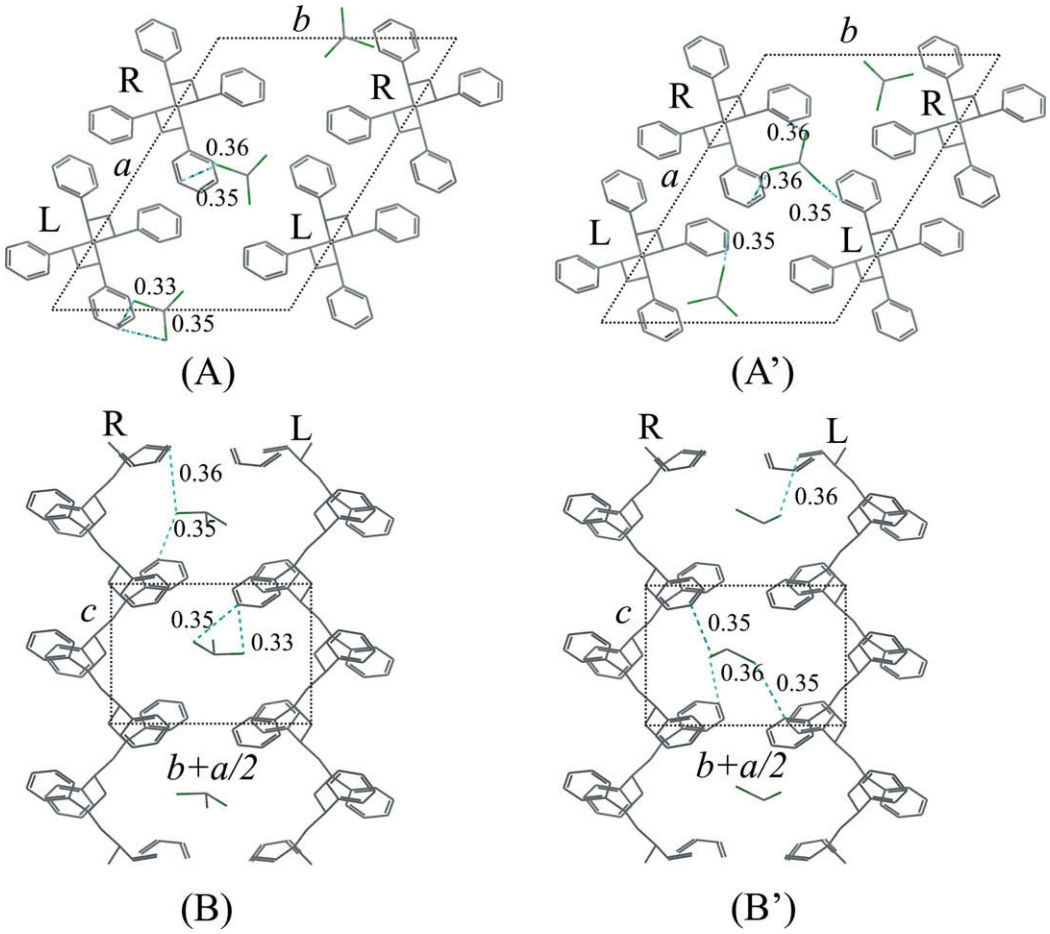

Fig. 3. Energetically equivalent packing models for the s-PS/$CHCl_3$ δ clathrate form as found by molecular mechanics calculation in the projections along *c* (A and A′) and along *c*(*b* + *a*/2) (B and B′). In (B) and (B′) only one couple of enantiomorphous polymer chains are shown. R = right-handed, L = left-handed helices. The shortest non-bonded distances (lower than 0.36 nm) between atoms are indicated in nm. The guest molecules have been represented in the cavities according both their possible centrosymmetrical arrangements.

mechanics calculations. The arrangement of the toluene/xylene molecule in the s-PS/toluene δ co-crystal according the structure proposed by Chatani et al. [2] is reported too for comparison. The different efficiency in the occupation of the cavities is apparent. Table 4 extends this comparison to all the δ clathrate forms whose crystal structure has been reported in the literature.

These data point out, as already stated in the literature [7,11], that depending on the steric requirements of the guest, the δ form can adapt itself by varying the volume of the cavity, even slightly modifying its shape. However, in every case reported in Table 4, the efficiency of the cavity volume occupation is always high (60–70%). The only exception is represented by the s-PS/$CHCl_3$ clathrate form for which the filling efficiency is decidedly lower (around 40%). In this case, in fact, the cavity generated by the chains seems to be much bigger than what we could expect from the guest volume. In our opinion, this unusual very low efficiency could be attributed to the not planar shape (tetrahedral) of the $CHCl_3$ molecule in respect to the other guest reported (all perfectly linear or planar [2–7,11]) that does not efficiently fit the "mostly planar" shape of the δ form cavity [30] (see Fig. 5). In this framework, may be useful to compare this clathrate with that formed with 1,2-dichloroethane (DCE). In order to accommodate chloroform guest molecule, in the process of the co-crystalline phase formation, the *ac* layers are compelled to stay at a greater distance in respect to δ form, leaving enough space to arrange the guest molecule in more than a way, as we have found by calculations. This is at variance with the case of DCE, a molecule having the same volume of $CHCl_3$ but a different shape, in which the *ac* layers even slightly approach [4].

Moreover it is worth noting that in both the minimum energy situation we have reported in Fig. 3, the guest molecule is arranged with the plane connecting the three chlorine atoms almost perpendicularly to the polymer chain axis (namely along the direction of maximum extension of the cavity) while the H atom is compelled to be fitted in towards the center of the cavity, where the thickness of the cavity is larger (see Fig. 5). If H atom is substituted by a bigger atom, as in the case of the carbon tetrachloride molecule, we expect that a similar arrangement of the guest molecule in the cavity would be not possible

Table 2
Fractional coordinates of the atoms of the asymmetric unit of the model of minimum energy for the s-PS/$CHCl_3$ δ clathrate form according the space group $P2_1/a$. Both the $CHCl_3$ guest molecules, corresponding to minimum energy models of Fig. 3, have been considered with an appropriate occupancy factor. Hydrogen atoms were included in the structure factors calculation, but they are omitted in this table for simplicity.

	x/a	y/b	z/c	o.f.[a]
C1	0.252	0.006	0.002	1
C2	0.230	0.076	0.130	1
C3	0.153	−0.006	0.251	1
C4	0.328	0.082	−0.126	1
C5	0.413	0.166	−0.029	1
C6	0.454	0.125	0.079	1
C7	0.531	0.203	0.168	1
C8	0.569	0.325	0.151	1
C9	0.529	0.368	0.042	1
C10	0.452	0.288	−0.046	1
C11	0.204	0.154	0.034	1
C12	0.134	0.108	−0.081	1
C13	0.111	0.180	−0.168	1
C14	0.158	0.303	−0.138	1
C15	0.229	0.351	−0.021	1
C16	0.251	0.277	0.063	1
C17	0.597	0.574	0.454	0.25
Cl1	0.709	0.623	0.504	0.25
Cl2	0.572	0.682	0.513	0.25
Cl3	0.524	0.437	0.555	0.25
C18	0.506	0.476	0.506	0.25
Cl4	0.430	0.504	0.400	0.25
Cl5	0.613	0.561	0.416	0.25
Cl6	0.467	0.323	0.500	0.25

[a] Occupancy factor.

Table 3
Comparison between observed structure factors (F_{obsd}), evaluated from the intensities reported in Table 1, and calculated structure factors (F_{calcd}) for the model of the s-PS/$CHCl_3$ δ clathrate form whose fractional coordinates are reported in Table 2. The Bragg distances, observed in the X-ray fiber diffraction pattern reported in Fig. 2A and calculated for the proposed monoclinic unit cell (a = 1.77 nm, b = 1.32 nm, c = 0.78 nm, γ = 121.5°), are also shown. Reflections not observed with F_{calcd} less than 20 have not been reported.

hkl	d_{obsd} (nm)	d_{calcd} (nm)	F_{obsd}	F_{calcd}	
010	1.07	1.13	48	35	
$2\bar{1}0$	0.87	0.87	86	65	
$2\bar{2}0$	0.57	0.64	40	35	36
020		0.56		10	
210	0.51	0.51	90	92	
$2\bar{3}0$		0.44		65	
$4\bar{2}0$	0.44	0.44	74	29	90
$4\bar{1}0$		0.43		54	
$4\bar{3}0$		0.38		54	
400		0.38		31	
030	0.38	0.38	61	40	82
220		0.37		36	
$6\bar{4}0$		0.27		47	
$4\bar{5}0$		0.26		15	
420	0.27	0.26	65	1	65
$2\bar{5}0$		0.26		25	
600		0.25		34	
$4\bar{4}0$	–	0.32	–	25	
040	–	0.28	–	30	
$1\bar{1}1$	0.65	0.66	51	32	
201		0.54		19	
111		0.54		115	
$1\bar{2}1$	0.52	0.50	150	99	160
$2\bar{2}1$		0.49		29	
$3\bar{1}1$		0.47		39	
$3\bar{2}1$	0.44	0.44	124	95	116
211		0.43		26	
301		0.42		62	
$2\bar{3}1$	0.38	0.38	99	34	120
$4\bar{2}1$		0.38		80	
$4\bar{1}1$		0.38		82	
$1\bar{4}1$	–	0.29	–	31	
$5\bar{4}1$		0.28		33	
$6\bar{2}1$	0.28	0.27	52	31	47
$6\bar{3}1$		0.27		1	
231		0.27		14	
$6\bar{1}1$	–	0.26	–	21	
$6\bar{4}1$	–	0.26	–	24	
$5\bar{5}1$	–	0.24	–	26	
$2\bar{5}1$	–	0.24	–	24	
$1\bar{1}2$		0.37		51	
012		0.37		44	
$2\bar{1}2$	0.36	0.36	109	64	101
202		0.35		1	
112		0.34		41	
022		0.32		6	
$3\bar{2}2$	0.32	0.32	90	47	82
$2\bar{1}2$		0.31		10	
302		0.31		66	
122		0.30		16	
$2\bar{3}2$	0.29	0.29	60	7	58
$4\bar{2}2$		0.29		18	
$4\bar{1}2$		0.29		53	
$4\bar{3}2$		0.27		61	
402	0.27	0.27	68	55	85
032		0.27		19	
222		0.26		8	
$5\bar{1}2$	–	0.26	–	33	
$5\bar{3}2$	–	0.25	–	23	
$4\bar{1}2$	–	0.24	–	31	

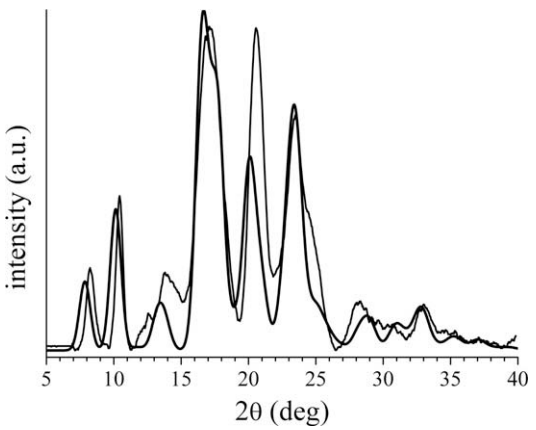

Fig. 4. Comparison between the experimental X-ray powder diffraction pattern (thin line) of the s-PS/$CHCl_3$ δ clathrate form after the subtraction of the amorphous halo reported in Fig. 2B with the calculated one (bold line) according to the structural model proposed in Fig. 3.

anymore without a further spacing of the *ac* layers, a fact that could make unstable the hypothetical clathrate structure. In order to support this hypothesis we have treated with CCl_4 amorphous and δ form samples of s-PS. No clathrate (or intercalate) structure has been obtained. It is worth

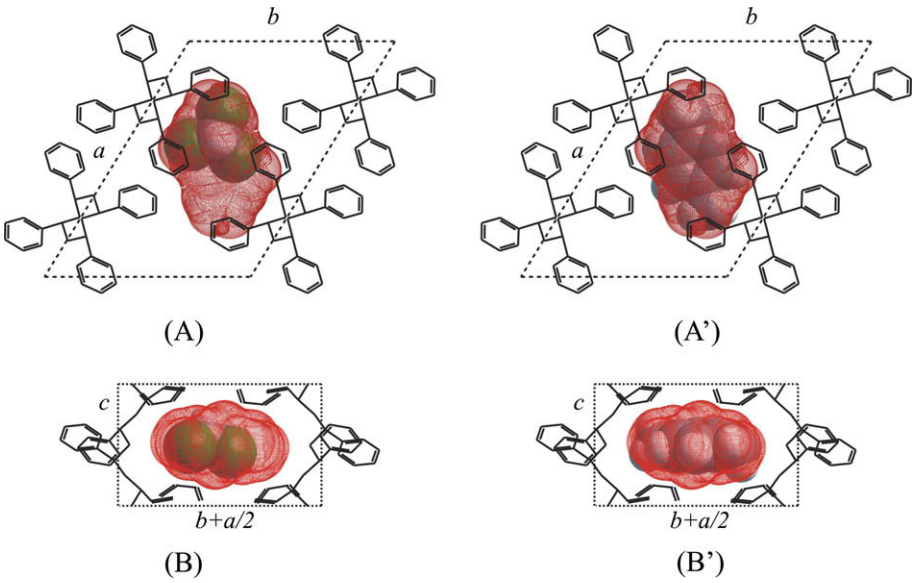

Fig. 5. (A and B) Schematic representations of the arrangement and of the space filling efficiency of the $CHCl_3$ guest molecule according one of the minimum energy models reported in Fig. 3. In (A′) and (B′) the same representations are presented for comparison for the case of the xylene guest molecule according the structure proposed by Chatani et al. [2]. Guest molecules are reported with their van der Waals radii. The cavities delimited by the helices have been indicated by the dotted regions calculated assuming a probe radius of 0.17 nm (equal to the van der Waals radius of Cl atom) according the Connolly method.

noting that for other "bulbous" guest molecules, such as [2.2.1]hepta-2,5-diene (norbornadiene) [9] or 2,2,6,6-tetramethylpiperidinyl-*N*-oxy (TEMPO) [23], only intercalate structures are known.

3.2. Arrangement of the chloroform guest molecules in the channels of the ε form

In a previous paper on the crystal structure determination of the s-PS nanoporous ε form, some of us reported preliminary calculations in order to reproduce an electronic diffraction pattern of the s-PS/$CHCl_3$ ε clathrate form [16]. These calculations have allowed individuating the situations of minimum energy to optimize the position of the $CHCl_3$ guest molecule inside the channels of that form. The results we have found indicate that there are several arrangements of the guest inside the channels but all having as a common feature a parallel orientation of the plane individuated by the three chlorine atoms almost parallel to polymer chain axis. This at variance with what we have

Table 4
Crystal structure parameters, volumes (of the unit cells, empty cavities and guest molecules) and cavity filling efficiency for some s-PS δ clathrate forms. Data for the nanoporous δ form are reported too.

δ Clathrate	Crystal structure parameters				Unit cell volume[a] ($nm^3 \times 10^{-3}$)	Empty cavity volume[b] ($nm^3 \times 10^{-3}$)	Guest volume ($nm^3 \times 10^{-3}$)	Cavity filling efficiency (%)
	a (nm)	*b* (nm)	*c* (nm)	γ (°)				
s-PS δ form [14]	1.74	1.19	0.77	117.0	1433	125	–	–
s-PS/$CHCl_3$	1.77	1.32	0.78	121.5	1554	185	73	39
s-PS/DCE [4]	1.71	1.22	0.77	120.0	1407	112	76	68
s-PS/toluene [2]	1.76	1.33	0.77	121.2	1555	186	104	56
s-PS/CS_2 [6]	1.73	1.27	0.79	120.0	1484	150	106[c]	70
s-PS/nitrobenzene [11]	1.80	1.32	0.78	122.0	1572	194	110	57
s-PS/*o*-DCB [7]	1.75	1.44	0.78	127.4	1562	189	117	62
s-PS/xylene[d]	1.76	1.33	0.77	121.2	1555	186	121	65
s-PS/*p*-nitroaniline [11][e]	1.80	1.29	0.78	122.3	1506	161	121	75
s-PS/I_2 [3]	1.73	1.29	0.78	120.3	1496	156	122[c]	78
s-PS/ethylbenzene [5]	1.77	1.34	0.80	121.7	1574	195	124	64

DCE = 1,2-dichloroethane; *o*-DCB = *ortho*-dichlorobenzene.

[a] In the unit cell volume calculation *c* has been considered equal to 0.78 nm for all the structures.

[b] Volumes of the hypothetical cavities generated by ignoring the presence of the guest molecules in each clathrate structure. It has been calculated as the difference between the unit cell volume and the volume of the chains calculated on the basis of the literature structure of the nanoporous δ form [14] with probe radius of 0.18 nm [30].

[c] For two guest molecules [3,6].

[d] The s-PS/toluene δ clathrate form unit cell parameters have been used [2].

[e] Actually, the s-PS/*p*-nitroaniline co-crystal presents a triclinic unit cell with constants $a = 1.795$ nm, $b = 1.29$ nm, $c = 0.78$ nm, $\alpha = 98°$, $\beta = 90°$ and $\gamma = 122.3°$ [11].

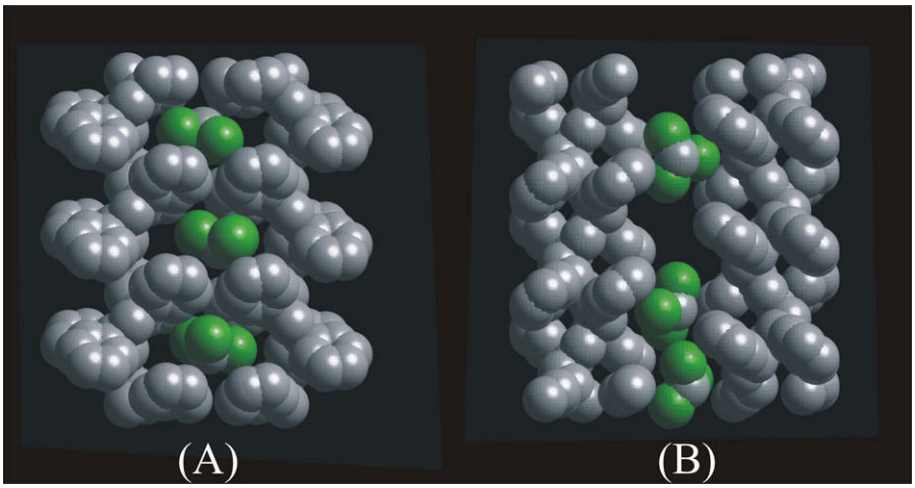

Fig. 6. Possible arrangements of the $CHCl_3$ guest molecules between one couple of polymer chains in the δ (A) and ε (B) type clathrate forms viewed according to the projections of Fig. 1B and B′, respectively. Three unit cells are shown along *c*. Guest molecules and polymer helices are reported with 0.7 times their van der Waals radii for the sake of the clarity.

found in the case of the s-PS/$CHCl_3$ δ clathrate for which the same planes are oriented almost perpendicularly to the chain axis. A comparison between these two different orientations has shown in Fig. 6. Further studies aiming at the complete structural characterization of the s-PS/$CHCl_3$ ε clathrate form are in progress.

4. Conclusions

The crystal structure of the δ clathrate form of s-PS containing $CHCl_3$ has been determined through X-ray diffraction analysis and molecular mechanics calculations. Preliminary results on the structure of the ε channel clathrate have been reported too. The δ clathrate presents, in analogy to all the other clathrate forms of s-PS determined up to now, an arrangement of the polymer helices forming isolated centrosymmetric cavities occupied by only one guest molecule despite the very large volume (nearly two times that of the $CHCl_3$ molecule) of the cavity. This corresponds to a low efficiency in the occupation of the cavity. The model is characterized by guest molecules that can statistically assume two energetically equivalent positions (and their centrosymmetrical ones) in the cavity corresponding to a disorder in the positioning of the guest molecules along the $b + a/2$ direction of the unit cell. In our opinion, this not efficient occupation of the space can be due to the not planar shape of the chloroform guest molecule. As far as the crystal structure of the ε clathrate, using the chain arrangement found for the nanoporous ε form in a previous work, some possible arrangements of the $CHCl_3$ molecules in its cavities have been suggested. The comparison between the two clathrates, δ and ε type, indicates that, in the case of the δ type co-crystals the planes passing for the three Cl atoms of each molecule are placed nearly perpendicularly to the chain axis while in the case of the ε type one they are nearly parallel to them, in agreement with what already found for planar molecules.

Acknowledgements

Financial support of the "Ministero dell'Istruzione, dell'Università e della Ricerca" (PRIN2007) and of the Consortium INSTM (PRISMA 01/2007) are gratefully acknowledged.

References

[1] Immirzi A, De Candia F, Iannelli P, Zambelli A, Vittoria V. Solvent-induced polymorphism in syndiotactic polystyrene. Makromolekulare Chemie Rapid Commun 1988;9(11):761–4.
[2] Chatani Y, Shimane Y, Inagaki T, Ijitsu T, Yukinari T, Shikuma H. Structural study on syndiotactic polystyrene: 2. Crystal structure of molecular compound with toluene. Polymer 1993;34(8):1620–4.
[3] Chatani Y, Inagaki T, Shimane Y, Shikuma H. Structural study on syndiotactic polystyrene: 4. Formation and crystal structure of molecular compound with iodine. Polymer 1993;34(23):4841–5.
[4] de Rosa C, Rizzo P, Ruiz de Ballesteros O, Petraccone V, Guerra G. Crystal structure of the clathrate δ form of syndiotactic polystyrene containing 1,2-dichloroethane. Polymer 1998;40(8):2103–10.
[5] Moyses S, Sonntag P, Spells SJ, Laveix O. Structural and morphological features of the syndiotactic polystyrene/ethylbenzene complex. Polymer 1998;39(15):3537–44.
[6] Tarallo O, Petraccone V. On the crystal structure of the clathrate forms of syndiotactic polystyrene containing carbon disulfide and iodine. Macromol Chem Phys 2004;205(10):1351–60.
[7] Tarallo O, Petraccone V. Syndiotactic polystyrene containing ortho-dichlorobenzene: crystal structure of the clathrate form. Macromol Chem Phys 2005;206(6):672–9.
[8] Petraccone V, Tarallo O, Venditto V, Guerra G. An intercalate molecular complex of syndiotactic polystyrene. Macromolecules 2005;38(16):6965–71.
[9] Tarallo O, Petraccone V, Venditto V, Guerra G. Crystalline structures of intercalate molecular complexes of syndiotactic polystyrene with two fluorescent guests: 1,3,5-trimethyl-benzene and 1,4-dimethyl-naphthalene. Polymer 2006;47(7):2402–10.
[10] Malik S, Rochas C, Guenet JM. Thermodynamic and structural investigations on the different forms of syndiotactic polystyrene intercalates. Macromolecules 2006;39(3):1000–7.
[11] Tarallo O, Petraccone V, Daniel C, Guerra G. Dipolar guest orientation in polymer co-crystals and macroscopic films. CrystEngComm 2009:2381–90.
[12] Milano G, Guerra G. Understanding at molecular level of nanoporous and co-crystalline materials based on syndiotactic polystyrene. Prog Mater Sci 2009;54(1):68–88.

[13] Gowd EB, Tashiro K, Ramesh C. Structural phase transitions of syndiotactic polystyrene. Prog Polym Sci 2009;34(3):280–315.
[14] De Rosa C, Guerra G, Petraccone V, Pirozzi B. Crystal structure of the emptied clathrate form (δ_e form) of syndiotactic polystyrene. Macromolecules 1997;30(14):4147–52.
[15] Rizzo P, Daniel C, De Girolamo Del Mauro A, Guerra G. New host polymeric framework and related polar guest cocrystals. Chem Mater 2007;19(16):3864–6.
[16] Petraccone V, Ruiz de Ballesteros O, Tarallo O, Rizzo P, Guerra G. Nanoporous polymer crystals with cavities and channels. Chem Mater 2008;20(11):3663–8.
[17] Guerra G, Milano G, Venditto V, Musto P, De Rosa C, Cavallo L. Thermoplastic molecular sieves. Chem Mater 2000;12(2):363–8.
[18] Daniel C, Alfano D, Venditto V, Cardea S, Reverchon E, Larobina D, et al. Aerogels with a microporous crystalline host phase. Adv Mater 2005;17(12):1515–8.
[19] Uda Y, Kaneko F, Tanigaki N, Kawaguchi T. The first example of a polymer-crystal-organic-dye composite material: the clathrate phase of syndiotactic polystyrene with azulene. Adv Mater 2005;17(15):1846–50.
[20] De Girolamo Del Mauro A, Carotenuto M, Venditto V, Petraccone V, Scoponi M, Guerra G. Fluorescence of syndiotactic polystyrene/trimethylbenzene clathrate and intercalate co-crystals. Chem Mater 2007;19(24):6041–6.
[21] Daniel C, Galdi N, Montefusco T, Guerra G. Syndiotactic polystyrene clathrates with polar guest molecules. Chem Mater 2007;19(13):3302–8.
[22] Stegmaier P, De Girolamo Del Mauro A, Venditto V, Guerra G. Optical recording materials based on photoisomerization of guest molecules of a polymeric crystalline host phase. Adv Mater 2005;17(9):1166–8.
[23] Kaneko F, Uda Y, Kajiwara A, Tanigaki N. Molecular-complex formation of syndiotactic polystyrene with stable radical molecules. Macromol Rapid Commun 2006;27(19):1643–7.
[24] Ibers JA, Hamilton WC. International tables for X-ray crystallography, vol. 4. Birmingham, England: The Kynoch Press; 1974.
[25] Sun H. COMPASS: an ab initio force-field optimized for condensed-phase applications-overview with details on alkane and benzene compounds. J Phys Chem B 1998;102(38):7338–64.
[26] Corradini P, Napolitano R, Pirozzi B. Geometrical and energetical analysis of the chain conformations of syndiotactic polystyrene in the crystalline state. Eur Polym J 1990;26(2):157–61.
[27] Daniel C, Menelle A, Brulet A, Guenet JM. Thermoreversible gelation of syndiotactic polystyrene in toluene and chloroform. Polymer 1997;38(16):4193–9.
[28] Mensitieri G, Larobina D, Guerra G, Venditto V, Fermeglia M, Pricl S. Chloroform sorption in nanoporous crystalline and amorphous phases of syndiotactic polystyrene. J Polym Sci B Polym Phys 2008;46(1):8–15.
[29] Musto P, Mensitieri G, Cotugno S, Guerra G, Venditto V. Probing by time-resolved FTIR spectroscopy mass transport, molecular interactions, and conformational ordering in the system chloroform-syndiotactic polystyrene. Macromolecules 2002;35(6):2296–304.
[30] Milano G, Venditto V, Guerra G, Cavallo L, Ciambelli P, Sannino D. Shape and volume of cavities in thermoplastic molecular sieves based on syndiotactic polystyrene. Chem Mater 2001;13(5):1506–11.